

A proposed architecture for lecithin cholesterol acyl transferase (LCAT): Identification of the catalytic triad and molecular modeling

F. PEELMAN,¹ N. VINAÏMONT,¹ A. VERHEE,² B. VANLOO,¹ J.-L. VERSCHELDE,² C. LABEUR,¹
S. SEGURET-MACE,³ N. DUVERGER,³ G. HUTCHINSON,⁴ J. VANDEKERCKHOVE,²
J. TAVERNIER,² AND M. ROSSENEU¹

¹Department of Biochemistry, Laboratory for Lipoprotein Chemistry, University of Gent, Gent, Belgium

²Flanders Interuniversity Institute for Biotechnology, Department of Biochemistry, University of Gent, Fac. Medicine, 9000 Gent, Belgium

³Rhône-Poulenc-Rorer-GENCELL, Cardiovascular Department, Vitry-sur Seine, France

⁴Department of Biochemistry, University College, London, United Kingdom

(RECEIVED September 16, 1997; ACCEPTED December 4, 1997)

Abstract

The enzyme cholesterol lecithin acyl transferase (LCAT) shares the Ser/Asp-Glu/His triad with lipases, esterases and proteases, but the low level of sequence homology between LCAT and these enzymes did not allow for the LCAT fold to be identified yet. We, therefore, relied upon structural homology calculations using threading methods based on alignment of the sequence against a library of solved three-dimensional protein structures, for prediction of the LCAT fold. We propose that LCAT, like lipases, belongs to the α/β hydrolase fold family, and that the central domain of LCAT consists of seven conserved parallel beta-strands connected by four α -helices and separated by loops. We used the conserved features of this protein fold for the prediction of functional domains in LCAT, and carried out site-directed mutagenesis for the localization of the active site residues. The wild-type enzyme and mutants were expressed in Cos-1 cells. LCAT mass was measured by ELISA, and enzymatic activity was measured on recombinant HDL, on LDL and on a monomeric substrate. We identified D345 and H377 as the catalytic residues of LCAT, together with F103 and L182 as the oxyanion hole residues. In analogy with lipases, we further propose that a potential "lid" domain at residues 50–74 of LCAT might be involved in the enzyme-substrate interaction. Molecular modeling of human LCAT was carried out using human pancreatic and *Candida antarctica* lipases as templates. The three-dimensional model proposed here is compatible with the position of natural mutants for either LCAT deficiency or Fish-eye disease. It enables moreover prediction of the LCAT domains involved in the interaction with the phospholipid and cholesterol substrates.

Keywords: catalytic residues; lecithin cholesterol acyl transferase; lipase; protein fold; threading

Lecithin cholesterol acyl transferase is an enzyme with different functions and a wide range of substrates. As its main activity, it hydrolyzes the sn-2 fatty acid of lecithin and transfers this fatty acid to cholesterol (Glomset, 1968). LCAT can, however, esterify other sterols (Kitabatake et al., 1979) and can further cleave the fatty acid chain of cholesteryl linoleate (Sorci-Thomas et al.,

1990), thereby acting as an enzyme of the cholesterol esterase family.

LCAT is active at the surface of both high and low density lipoproteins, with a corresponding α and β activity (Jonas, 1991). The α -activity of LCAT on HDL requires the presence of apolipoprotein AI or apo AIV as co-factor, while these co-factors are not involved in β -activity. Several mutations in the LCAT gene, which underlie either Familial LCAT Deficiency (FLD) or Fish-Eye Disease (FED), have recently been reviewed (Kuivenhoven et al., 1997). FLD is characterized by a virtual absence of plasma LCAT activity, while β -activity is retained in FED. Both FLD and FED patients develop corneal opacity and hypolipoproteinemia, while FLD patients often suffer from renal disease. Recent studies in transgenic rabbits (Hoeg et al., 1996) and in mice infected by an adenovirus carrying the LCAT gene (Séguret-Macé et al., 1996)

Reprint requests to: Maryvonne Rosseneu, Department of Biochemistry, Laboratory of Lipoprotein Chemistry, University of Gent, Hospitaalstr. 13, 9000 Gent, Belgium; e-mail: maryvonne.rosseneu@rug.ac.be.

Abbreviations: LCAT, lecithin cholesterol acyl transferase; r-HDL, reconstituted HDL consisting of 1-palmitoyl-2-linoleoyl phosphatidylcholine/cholesterol/apo A-I at a molar ratio of 100/10/1; LDL, low density lipoprotein; monomeric substrate, 1,2-bis-(1-pyrene-butanoyl)-sn-glycero-3-phosphocholine.

have shown that increased LCAT concentrations and activity in these animals are associated with changes in their plasma HDL profiles. These data have emphasized the importance of LCAT in modulating the plasma HDL levels and consequently in increasing the protective action of these lipoproteins against cardiovascular disease (Séguret-Macé et al., 1996).

Although it was suggested that LCAT shares the nucleophile/acid/histidine catalytic triad with lipases and esterases (Jauhiainen & Dolphin, 1986, 1991; Jauhiainen et al., 1987), only the catalytic nucleophile residue Ser181 has been identified so far (Francone & Fielding, 1991). Due to the high level of conservation between sequences of different LCAT species, the histidine and acid (Asp or Glu) active site residues are difficult to localize. The low level of sequence homology between LCAT, lipases, and esterases did not allow the LCAT fold to be identified. We, therefore, used a threading approach, based on alignment of the sequence against a library of solved three-dimensional (3D) protein structures, for prediction of the LCAT fold, and suggest here that LCAT, like lipases, belongs to the α/β hydrolase fold family. As suggested by Ollis and coworkers (Ollis et al., 1992), the α/β hydrolase fold family represents a clear example of the structural conservation of a catalytic subsite architecture during the evolution of enzymes with different activities and substrates. In this fold, the core of each enzyme consists of a central β sheet, made of parallel strands, and sandwiched between two layers of α -helices. The central β strands are thus connected through the α -helices, and separated by variable extensions or loops (Ollis et al., 1992). In this particular configuration, the nucleophile, acid, and histidine active site residues are separated by only a few Å in the 3D structure of the enzyme. We used the conserved features of this protein fold for the prediction of functional domains in LCAT, as this approach had been successfully applied to the central domain of the bacterial enhancer-binding proteins (Osuna et al., 1997) and to the ferrocyclase family of proteins (Hansson et al., 1997). As recently described for three lipases (Lhose et al., 1997), knowledge of the general topology of the enzyme is quite helpful for a first selection of the candidate active site residues. We, therefore, relied on the structural homology with lipases and on the α/β hydrolase fold, predicted for LCAT, in order to limit the number of point mutations, necessary to identify the active site acid and histidine residues, and the oxyanion hole residues of LCAT. A molecular model of LCAT would be a useful tool for structure-function analysis of the enzyme, and would help understanding the wide substrate specificity and the combined phospholipase and acyl transferase activity of LCAT. We, therefore, built a 3D model by molecular modeling, for the core and catalytic triad of LCAT, using as templates the homologous lipases predicted by threading. In the proposed model, the spatial configuration of the catalytic residues is typical for a protein with an α/β hydrolase fold. This model should prove useful for the design and testing of LCAT mutants with specific substrate activity (Rosseneu et al., 1997).

Results

Search for a folding pattern

A multiple sequence alignment of the human, baboon, rabbit, rat, mouse, and chicken LCAT, generated by the CLUSTAL program (Higgins & Sharp, 1988) shows that the degree of sequence conservation between human, baboon, rabbit, rat, and mouse LCAT reaches above 85%, while chicken LCAT is conserved around 75%

compared to the other species (Hengstschlager-Ottstad et al., 1995). This multiple sequence alignment was used as input for several secondary structure prediction programs (see Materials and methods). The results suggest, with a high degree of reliability as estimated by the PHD server, that LCAT should consist of 12 β -strands, 6 helices, and 24 β -turns, identified using the GORBTURN program (Wilmot & Thornton, 1988).

Using the BLAST algorithm (Altschul et al., 1990), we searched for sequence similarity between LCAT and the proteins of the SwissProt databank. The only protein with high enough homology (31%) to yield a meaningful sequence alignment was the new 75.4 kD hypothetical protein, homologous to mammalian LCAT, recently identified in yeast (Verhasselt et al., 1994). The CLUSTAL alignment of the entire LCAT sequence with residues 150–661 of the yeast protein suggests that there is sequence conservation around Ser181 of LCAT and Ser324 of the yeast protein, as well as conservation of the Cys residues linked by a disulfide bridge, at positions 50–74 and 313–356 in LCAT and 197–223 and 526–567 in the yeast protein (data not shown). Serine carboxypeptidase II and cutinase, i.e. two enzymes belonging to the α/β hydrolase family, were further identified by a BLAST search of the PDB data bank, although with a lower level of sequence homology with LCAT.

In order to search for structural homology between LCAT and other crystallized proteins, the sequence of human, baboon, rabbit, rat, mouse, and chicken LCAT were threaded against the database of protein structures. According to the THREADER program (Jones et al., 1992, 1995), three out of the 15 proteins with the highest homology scores with human LCAT have an α/β hydrolase fold, while five others display a similar three-layer architecture, consisting of a combination of α -helices covering a central β -sheet (Table 1A). Two of the proteins with an α/β hydrolase fold are lipases: *Candida antarctica* lipase and *Fusarium solani* cutinase, while the third protein is *Xanthobacter autotrophicus* dehalogenase. This algorithm often identifies neuraminidase among the top scores proteins, and this information is probably not relevant for LCAT (D.T. Jones, pers. comm.). According to the 123D threading algorithm (Alexandrov et al., 1996), *Torpedo californica* acetylcholinesterase, human pancreatic lipase, and *Candida rugosa* lipase belong to the 20 best fitting structures to the human LCAT sequence (Table 1B). A fold-recognition using sequence-derived predictions was also performed using the 3D profile algorithm (Fisher & Eisenberg, 1996). This program predicted an α/β hydrolase fold for LCAT as well, and identified pancreatic lipase among the ten homologous proteins with the highest scores (data not shown). Threading of the other LCAT species using the THREADER program further predicts similarity of rat LCAT with the α/β hydrolase fold of *Humicola lanuginosa* lipase and of rabbit and chicken LCAT with thioesterase from *Vibrio harveyi* (data not shown). The 123D algorithm predicts that LCAT from different species have the same structural homology as human LCAT. The alignment of the human LCAT sequence around the active site S181 (residues 150–210), with sequences of other α/β hydrolases predicted by THREADER and 123D is shown in Figures 1A and B. These results clearly demonstrate that S181, previously identified as the active site nucleophile of LCAT (Francone & Fielding, 1991), aligns with the active site nucleophile of the other α/β hydrolase enzymes. Among all proteins predicted by the two threading methods to be structurally homologous to LCAT (Table 1), only those with an α/β hydrolase fold, aligned properly around the active site Ser of LCAT. Lipases are characterized by a conserved structural β -eSer- α motif around the active site serine.

residues 175–178, of the active site Ser181, the α 5–6 helix at 182–193, and of strand six at residues 206–210 in LCAT (Fig. 1).

As discussed by Jones (Jones et al., 1995), the THREADER program is powerful enough to detect high scoring local alignments, while the 123D method can align longer stretches of sequences with better reliability. The alignment of the LCAT N-terminal domain with *Candida rugosa* lipase, obtained from the 123D program, is shown in Figure 2A. In spite of the low level of sequence homology between the two enzymes (<25%), the 123D algorithm predicts good correspondence between the secondary structure elements. Besides the central conserved elements described above (Fig. 1), the alignment further predicts strands β 2 at residues 79–84, β 3 at 97–100 and the helix α 3–4 at 116–129 in human LCAT. The alignment of the N-terminal residues of LCAT with residues 1–180 of human pancreatic lipase, derived by the 123D threading procedure (Alexandrov et al., 1996), is shown in Figure 2B. In agreement with *Candida rugosa* lipase (Fig. 2A), the sequence alignment with human pancreatic lipase predicts β 3 at residues 97–100 and helix α 3–4 at 116–129 in LCAT. However, strand β 2 at residues 79–84 of LCAT does not align with β 2 at

residues 51–53 in human pancreatic lipase, probably due to the particular topology of the N-terminal domain of this lipase, spanning residues 1–150, as: $-1, +3, -1x, +2x, +1x$.

A typical α/β hydrolase fold is depicted in Figure 3A. In this fold, the core of each enzyme is similar: an α/β sheet consisting of β -strands connected by α -helices and separated by variable extensions or loops (Ollis et al., 1992). Conserved central elements between strands three and seven include: α -helix 4–5, preceding β -strand 5 which is immediately followed by the active site nucleophile in a sharp γ -turn, or "nucleophile elbow." The active site Ser is followed by helix 5–6 and β -strand 6. The acid active site residue is positioned at the end of β -strand seven, in the middle of two reverse turns, while the position of the active site His residue, C-terminal of strand eight is more variable. Based on this particular configuration, the active site residues are separated by only a few Å in the 3D structure of the enzyme. In lipases, the oxyanion hole residues, which contribute to the stabilisation of the intermediate oxyanion during the enzymatic reaction, are spatially close to the catalytic triad residues (Van Tilbeurgh et al., 1993). Less conserved elements consist of excursions or loops mainly between

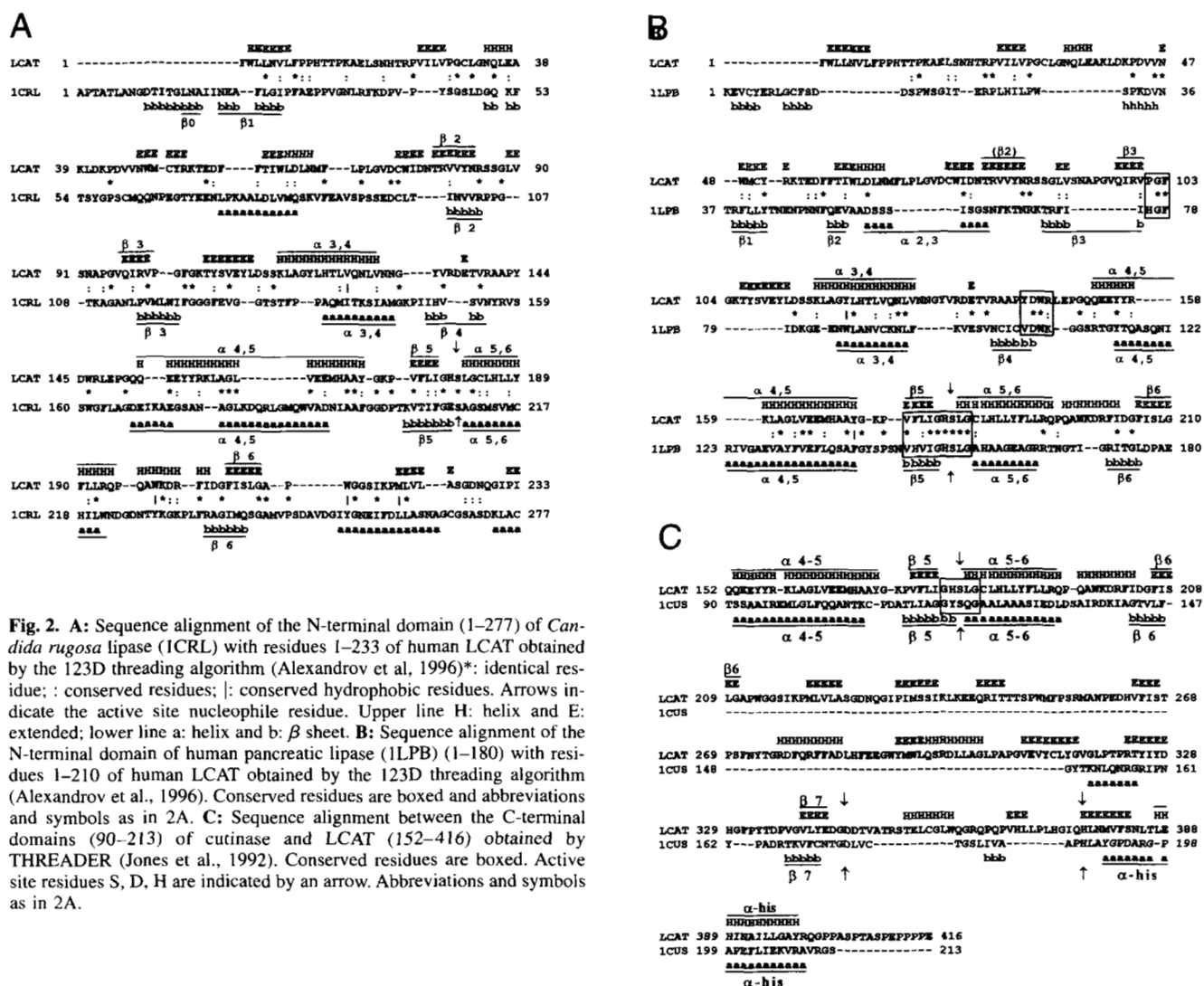


Fig. 2. A: Sequence alignment of the N-terminal domain (1–277) of *Candida rugosa* lipase (ICRL) with residues 1–233 of human LCAT obtained by the 123D threading algorithm (Alexandrov et al., 1996)*: identical residue; : conserved residues; |: conserved hydrophobic residues. Arrows indicate the active site nucleophile residue. Upper line H: helix and E: extended; lower line α : helix and β : β sheet. B: Sequence alignment of the N-terminal domain of human pancreatic lipase (ILPB) (1–180) with residues 1–210 of human LCAT obtained by the 123D threading algorithm (Alexandrov et al., 1996). Conserved residues are boxed and abbreviations and symbols as in 2A. C: Sequence alignment between the C-terminal domains (90–213) of cutinase and LCAT (152–416) obtained by THREADER (Jones et al., 1992). Conserved residues are boxed. Active site residues S, D, H are indicated by an arrow. Abbreviations and symbols as in 2A.

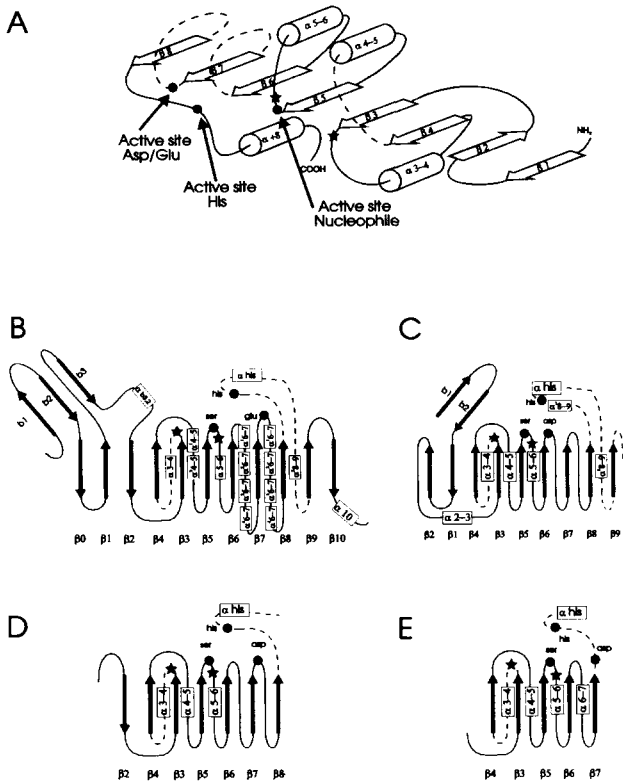


Fig. 3. Schematic diagram of the topology of the α/β hydrolase fold. A: 3D representation of the α/β hydrolase fold (Ollis et al., 1992). B: *Candida rugosa* lipase. C: Pancreatic lipase. D: Predicted topology of LCAT showing the conserved β -strands, α -helices, and the position of the catalytic and oxyanion hole residues. E: Cutinase.

strands 6 and 7. These variable loops are involved in substrate specificity of the different enzymes of the family. The topology of the *Candida rugosa* lipase (Fig. 3B) is typical for the α/β hydrolase fold and can be represented by the notation: +1, +2, -1x, +2x, 4(+1x), +1, ignoring the first strand (Richardson, 1981; Ollis et al., 1992). The topology of human pancreatic lipase (-1, +3, -1x, +2x, 3(+1x)) (Fig. 3C) differs from the normal α/β hydrolase topology, in the sequence domain connecting strands 1 and 3. This particular fold can, however, be converted into the more conventional α/β hydrolase topology of the *Candida rugosa* lipase by deletion of residues 47-63, including strand $\beta 2$ and helix $\alpha 2-3$. In order to match the predicted structural motives of LCAT with both the human pancreatic and *Candida rugosa* lipases identified by threading, we manually aligned the LCAT sequence with that of human pancreatic lipase after introduction of a gap at residue 88 of LCAT, to account for the extra residues 47-63 of pancreatic lipase (Fig. 4). This new alignment identifies strand $\beta 4$ at residues 141-146 of LCAT. The alignment of the N-terminal domain of LCAT with several members of the lipoprotein, hepatic, and pancreatic lipase superfamily (Hide et al., 1992) clearly demonstrates that there is significant sequence identity between the conserved structural elements of the α/β hydrolase fold in LCAT and in the other lipases (Fig. 4). These residues include NTR, N-terminal of strand $\beta 2$, and VPGF at the end of $\beta 3$. The latter residues include the conserved G preceding the oxyanion hole residue F. Identical residues further include YDW at the end of $\beta 4$

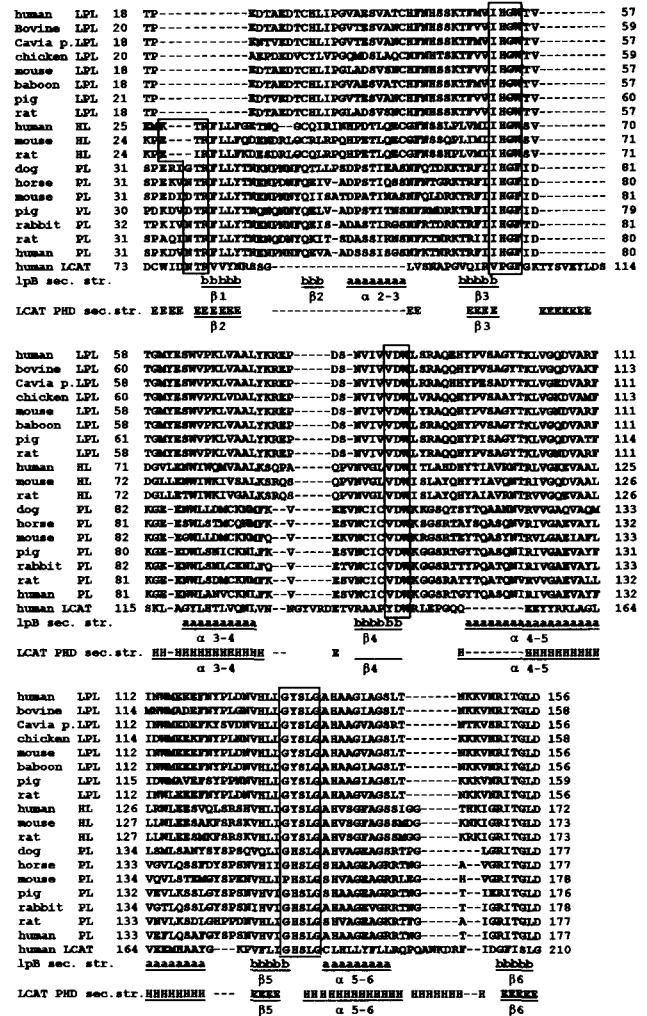


Fig. 4. Multiple sequence alignments of the hepatic, lipoprotein, and pancreatic lipase superfamily (Hide et al., 1992) with human LCAT (73-210), including the gap manually introduced at residue 88 of LCAT to compensate for the residues 46-64 of pancreatic lipase. Homologous residues in lipases and LCAT are boxed and structural elements (a, H: helix; b, E: strand) identified in lipases and predicted in LCAT using the PHD program are underlined.

and finally the GHSLG motif, which includes both the active site S and the second oxyanion hole L in LCAT. In the lipase superfamily, only these residues are strictly conserved in the N-terminal part of the sequence. These are probably crucial for the proper arrangement of the strands of the core β -sheet both in lipases and in LCAT. These conserved elements were also identified in the new 75.4 kD hypothetical protein, identified in yeast (data not shown). The resulting topology for LCAT, shown in Figure 3D, is: +2, -1x, +2x, 3(+1x), in agreement with that of *Candida rugosa* lipase. According to the proposed topology, all conserved residues between LCAT and lipases are located in the upper part of the molecule on top of the central β -sheet, in the neighborhood of the active site S181 (Fig. 3D).

As the sequences of the human pancreatic and *Candida rugosa* lipases contain long excursions and loops C-terminal of strand 6, the alignment of these sequences with LCAT, obtained either by the THREADER or 123D programs, is little informative. In con-

trast, the alignment of the LCAT sequence with cutinase obtained by THREADER (Fig. 2C) shows highest homology between structural elements in the C-terminal domain of the two enzymes. This is observed around the active site Ser residue at position 181 in LCAT and 120 in cutinase, of strand six at residues 206–210 of LCAT with $\beta 6$ in cutinase, of a putative strand seven predicted in LCAT at residues 339–342 by the PHD program, with $\beta 7$ in cutinase. The cutinase topology, shown in Figure 3E, is $-1x, +2x, 2(+1x)$. Moreover, the active site residues D175 and H188 of cutinase align with D345 and H377 in LCAT. In the two enzymes, as in most lipases, this histidine residue is followed by an α -helical segment, termed α -His. The alignment of the two sequences includes a large gap at residue 147 of cutinase, corresponding to residues 208–314 of the long excursion between strands 6 and 7 of LCAT (Fig. 2C). Another feature of the α/β hydrolase fold is the conservation of hydrophobic residues on the face of the β -strands constituting the core of the protein. This is illustrated in Figure 5A for the hydrophobic residues in the proximal face of the LCAT strands, compared to those of human pancreatic lipase, *Candida rugosa* lipase, and *Fusarium solani* cutinase, further corroborating the predicted structural homology. These hydrophobic residues are in close proximity to those of the hydrophobic face of the helices covering the central β -sheet. Arrangement of the hydrophobic and hydrophilic residues in the helices $\alpha 3$ –4, $\alpha 4$ –5, $\alpha 5$ –6, and α -His of LCAT is depicted in an Edmundson-wheel representation in Figure 5B. This figure illustrates the amphipathicity of the LCAT

helices, whose hydrophobic face shield the hydrophobic core residues of the structural central β -sheet, consisting of strands 2–7 (Fig. 5A).

Site-directed mutagenesis of human LCAT

In order to identify the catalytic residues of human LCAT, we relied upon one of the conserved features of the α/β hydrolase fold, i.e., that catalytic triad residues always occur in the same order in the primary sequence: nucleophile, acid, histidine (Ollis et al., 1992) and mutated successively the His and carboxylic acid residues, C-terminal of S181.

Site-directed mutagenesis of the His residues

We first mutated the His residues occurring C-terminal of S181, which are fully conserved in the six sequenced LCAT species: human, baboon, rabbit, rat, mouse, and chicken. Three conserved candidate His residues were identified at positions 263, 368, and 377, and mutated to an alanine. Immunoblots of the culture media demonstrated the expression of the WT and mutant proteins with identical molecular weight (data not shown). The expression level measured by ELISA was around $2 \mu\text{g}/\text{mL}$ medium for WT LCAT, while the His-Ala mutants were expressed at 50–70% of the WT enzyme (Table 2). The specific activity of the H263-A mutant was comparable to that of WT LCAT on all substrates, whereas the H368-A mutant had comparable activity on LDL but strongly decreased activity on r-HDL, similar to FED mutants (Kuivenhoven et al., 1997). The H377-A mutant was expressed at a 70% level compared to WT LCAT, but it lost both acyl transferase activity on an organized lipid substrate, and phospholipase activity on a monomeric substrate (Table 2). This residue is the only His conserved in all LCAT species, which occurs C-terminal of S181, and which lost 100% activity when mutated to an Ala. These data, therefore, strongly suggest that H377 represents the catalytic site His residue of human, baboon, rabbit, rat, mouse, and chicken LCAT.

Site-directed mutagenesis of the acid residue of the catalytic triad

For the identification of the acid residue of the LCAT catalytic triad, we relied upon the results of the secondary structure prediction and threading programs described above, which suggest that LCAT belongs to the lipase family. We first examined which subclasses of lipases include either an Asp or a Glu in their catalytic triad. Aspartic acid is the catalytic residue in most lipases, as Glu occurs only in the catalytic triad of the carboxylesterases of the Type B family (Cygler et al., 1993). Proteins of this family are more distantly related to human plasma LCAT than, for example, hepatic and lipoprotein lipases which have an Asp catalytic residue. As a first selection for mutagenesis, we, therefore, considered the Asp residues located between S181 and H377, which are conserved in all LCAT species, i.e., D200, 227, 262, 277, 284, 298, 328, 335, 343, 345, and 346. A further, more restrictive selection of the candidate Asp residues was based upon the observation that, except for bacterial lipases, the active site Asp is located at the end of strand six or seven in all lipases. Using a combination of these two selection criteria, only D227, 328, 335, 343, 345, and 346 remained as candidates for the acid active site residue of LCAT. These Asp were separately mutated to an Asn residue. Immunoblots, together with the ELISA mass assays (Table 2), demonstrate

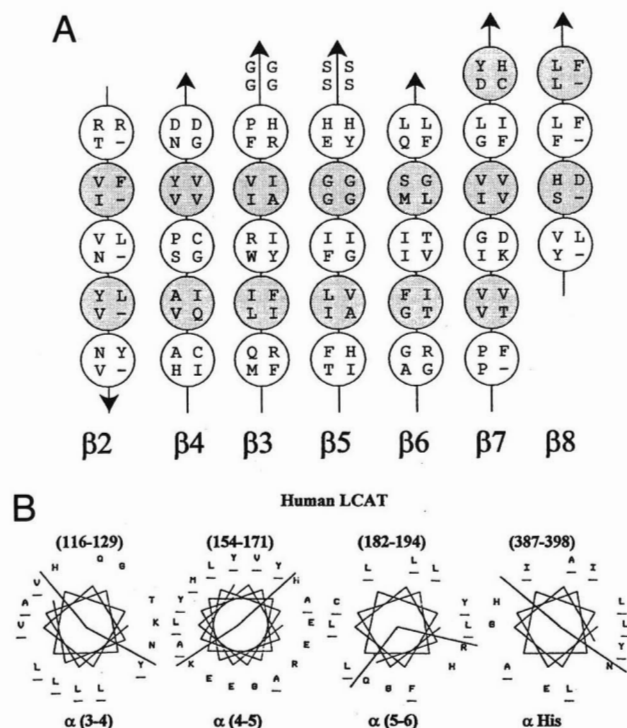


Fig. 5. A: Residues distribution on the proximal β -strands of the α/β hydrolase fold. Each circle contains a residue of LCAT (upper left), human pancreatic lipase (upper right), *Candida rugosa* lipase (lower left), and *Fusarium solani* cutinase (lower right). Shaded circles indicate residues on the proximal side of the β sheet, facing helices α (4–5) and α (5–6). **B:** Edmundson-wheel representation of the residues of the central helices of human LCAT. Hydrophobic residues are underlined and residue numbers are indicated above each helical wheel.

Table 2. Mass and specific activity (\pm SD) of media from mutant and wild-type LCAT transfectants ($n = 3$)

Transfectant	Mass ($\mu\text{g}/\text{mL}$)	Specific activity		
		r-HDL (nmol CE/ μg LCAT/h)	LDL (nmol CE/ μg LCAT/h)	Monomeric substrate % of WT
Wild-type	2.3 \pm 0.5	4.4 \pm 1.3	0.6 \pm 0.1	100
H263-A	1.5 \pm 0.3	5.2 \pm 0.8	0.5 \pm 0.2	84 \pm 16
H368-A	1.1 \pm 0.1	1.4 \pm 0.9	0.9 \pm 0.4	50 \pm 11
H377-A	1.6 \pm 0.3	0	0	0
D227-N	1.9 \pm 0.6	4.0 \pm 0.6	0.5 \pm 0.1	99 \pm 15
D328-N	1.6 \pm 0.4	4.7 \pm 0.6	0.3 \pm 0.1	55 \pm 10
D335-N	1.4 \pm 0.2	4.7 \pm 0.7	0.2 \pm 0.05	69 \pm 13
D343-N	0.9 \pm 0.2	3.6 \pm 0.5	0.1 \pm 0.05	12 \pm 5
D345-N	1.6 \pm 0.2	0	0	0
D346-N	1.1 \pm 0.2	6.5 \pm 1.3	0.4 \pm 0.1	126 \pm 16
G102-L	2.1 \pm 0.2	0.02 \pm 0.1	0	0
W61-F	2.7 \pm 0.5	4.1 \pm 0.6	0.8 \pm 0.2	164 \pm 18
W61-L	3.1 \pm 0.8	0	0.7 \pm 0.1	20 \pm 8
W61-G	2.9 \pm 0.6	0	0.6 \pm 0.1	18 \pm 7
del 50-74	2.2 \pm 0.4	0	0	0

that all mutants have the same molecular weight as WT LCAT, and are secreted at levels varying between 0.9 and 1.8 $\mu\text{g}/\text{mL}$ into the cell medium. Only the D345-N mutation produced an enzyme which had lost activity on the three LCAT substrates. The D343-N mutant retained activity on r-HDL while losing 80% activity on LDL and on the monomeric substrate, suggesting that this mutation probably affects the local conformation of the protein. These data, therefore, suggest that D345 belongs to the catalytic triad of human LCAT.

Site-directed mutagenesis of the oxyanion hole residues of human LCAT

The position of the oxyanion hole residues is strictly conserved in the enzymes with an α/β hydrolase fold (Ollis et al., 1992). In lipases, one of the oxyanion hole residues is at position +1 of the active site Ser, thus predicted as L182 in all LCAT species, except for M182 in chicken LCAT. The other oxyanion hole residue is located C-terminal of strand three, and it is preceded by a conserved glycine, to enable the backbone amides of the oxyanion hole residues to point toward the nucleophile. The sequence alignment and secondary structure prediction for all LCAT species, together with the alignment between LCAT, lipoprotein, hepatic, and pancreatic lipase sequences (Fig. 4) predicts that F103 is the second oxyanion hole residue of LCAT. Site-directed mutagenesis of L182 would not be informative, as the vicinity of the active site S181 would be critical to any mutation introduced there. In order to confirm the role of F103 as the second oxyanion hole residue, we mutated the conserved G102 residue at position -1 of F103, to Leu. The mutation of a small mobile Gly residue to a more bulky Leu was designed to cause steric hindrance and prevent the backbone amide of F103 to point toward S181 and L182. The G102-L mutant was expressed at the same level as WT LCAT, but lost activity on all substrates (Table 2), as predicted by the proposed model. These data thus support the hypothesis that F103 is one of the oxyanion hole residues of LCAT.

Site-directed mutagenesis of a putative "lid" domain

Another conserved feature between most lipase members of the α/β hydrolase fold family is the occurrence of a "lid" or "flap," which is a highly mobile segment covering the hydrophobic active site of the enzyme in its closed conformation (Ollis et al., 1992). Such a lid was first identified in the 3D structure of human pancreatic lipase (Winkler et al., 1990; Van Tilbeurgh et al., 1993), and has been deduced by homology for the lipoprotein and hepatic lipases (Hide et al., 1992; Van Tilbeurgh et al., 1993). Lids often consist of 20–25 residue segments, closed by a disulfide bridge between two cysteines at their N- and C-terminal ends. Within the lipase family, they are located in loops at variable positions in the sequence; in fungal lipases, the lid lies N-terminal of the active site Ser residue, while it is located between the active site Asp and His residues in the pancreatic, hepatic, and lipoprotein lipases. A most likely candidate for a lid structure in LCAT is the 50–74 segment between C50 and C74, as these residues were shown to form a disulfide bridge (Yang et al., 1987). The threading alignment (Fig. 2A) further suggests that C50 and C74 of LCAT should correspond with C60 and C97 of *Candida rugosa* lipase, which close the lid domain of this enzyme through a disulfide bridge, as in LCAT. Moreover, the central part of this domain has homology to the hepatic and pancreatic lipases lids, and W61 of LCAT would correspond to W252 in human pancreatic lipase (Van Tilbeurgh et al., 1993). A Trp residue occurs in several lipase lids and was shown by site-directed mutagenesis of the *Humicola lanuginosa* lipase to bind the cleaved long chain fatty acid, in the active site of the enzyme (Martinelle et al., 1996).

To test this prediction, we deleted the C50–C74 domain of LCAT and we mutated the W61 residue to either F, L, or G, in analogy with mutations of the *Humicola lanuginosa* lipase (Martinelle et al., 1996). The W61-F substitution had little effect on the enzymatic activity on the lipoprotein substrates and even increased the enzymatic activity on the monomeric substrate. The W61-L and W61-G mutations decreased the enzymatic activity on the

monomeric substrate and abolished activity on r-HDL, while the C50-C74 deletion mutant had no residual activity on either substrate (Table 2). These data thus suggest that an aromatic residue (W and F) at position 61 contributes to the interaction of the enzyme with its substrate. In analogy with other lipases, the 50–74 domain of LCAT seems a good candidate for a putative “lid” in this enzyme.

Model building and biological implications

The results obtained by site-directed mutagenesis and the activity measurements of the LCAT mutants thus support the α/β hydrolase fold (Fig. 3), predicted by threading. In agreement with the conserved elements of this fold, the active site S181 in LCAT is located in a sharp turn C-terminal of the strand five, while D345 is found after strand seven, in a double β -turn, and H377 is followed by an α -helix (Fig. 3). The oxyanion hole residues F103 and L182 lie C-terminal of strand three and at position +1 of the active site Ser, respectively. The long excursion at residues 211–314, between strand six and seven of LCAT, might be involved in the enzyme-substrate recognition. It is predicted to consist of one helix and four β -strands, according to the PHD program. We did not model the 17 carboxy-terminal residues of LCAT, which are absent in the chicken LCAT sequence. In the other LCAT species, this stretch of residues contains five to six prolines and probably has a disordered structure. Cleavage of the C-terminal residues does not seem to decrease the enzymatic activity of LCAT (Francone et al., 1996; Lee et al., 1997).

This model is further supported by residue conservation around the active site S181, D345, and the oxyanion hole residue F103 of LCAT, with other lipases (Fig. 6). Although the residues around the active site Asp residue of lipases are not as strictly conserved as those around the nucleophile Ser (Fig. 6A), there is structural homology around D345 of LCAT with several α/β -hydrolases containing an active site Asp (Fig. 6B). Figure 6B shows conservation of β 7 preceding the active site Asp (indicated by an arrow), of the two reverse turns with the Asp as junction residue, and of the hydrophobic residues (boxed) at position +2 and +3 of the active site Asp. These features were also predicted for the new 75.4 kD hypothetical protein, homologous to mammalian LCAT, recently identified in yeast (Verhasselt et al., 1994). The third residue of the catalytic triad, identified as H377, aligns with H188 of cutinase (Fig. 2C). According to the PHD predictions, this residue is, moreover, followed by an α -helix at residues 387–398, as in cutinase and in several other lipases. The sequence conservation around the oxyanion hole residue F103 of LCAT, with the corresponding residue of other α/β -hydrolases is illustrated in Figure 6C, showing conservation of the preceding Gly residue.

After identification of the different structural elements described above, we attempted to build a 3D model for LCAT, using the Biosym HOMOLOG software. The N-terminal domain of LCAT, between residues 73 and 210, was built using the manual alignment and the coordinates of human pancreatic lipase (Fig. 7), as a template (Egloff et al., 1995). Pancreatic lipase was selected as template, as highest residue conservation was found between LCAT and this lipase. We could not construct the N-terminal domain preceding residue 73, since residues 1–50 of LCAT share only weak homology with other lipases. Moreover, C31 and 184 should be spatially close in LCAT (Jauhainen et al., 1988; Yang et al., 1987), thereby fixing the position of the loop at C50–C74, for which we had no template. Building the C-terminal part of LCAT

(residues 333–399) required as template a lipase whose active site Asp would follow β 7, and not β 6, as is the case for pancreatic lipase. *Candida antarctica* lipase (residues 177–242) was selected as the best candidate, based upon the high secondary structure homology of the C-terminal domain of this enzyme with the predicted structural and functional elements of LCAT. For example, strands β 7 and β 8, and the C-terminal helix of LCAT were correctly aligned with corresponding elements of this lipase, while the active site residues D345 and H377 of LCAT aligned with D187 and H224 of *Candida antarctica* lipase. Cutinase was not an appropriate template for the C-terminal domain of LCAT, as its active site D175, unlike D345 in LCAT, is located within a disulfide bridge at C171–178. We did not model the excursion at residues 210–332 of LCAT, due to lack of an appropriate template. The resulting working model (Fig. 7) possesses a structural topology consistent with, but not identical to, *Candida rugosa* lipase. The structural topology consists of a central β -sheet consisting of one anti-parallel (β 2) and six parallel (β 3–8) strands: 2 (R80–N84), 3 (Q97–P101), 4 (A141–W146), 5 (F176–H180), 6 (G205–L209), 7 (336–Y341), 8 (V367–L370). The central β -sheet is surrounded by four helices: α 3–4: (K116–V129), α 4–5: (D154–Y171), α 5–6: (L182–Q194), α -His: (L387–Y398). As in the α/β hydrolase fold of lipases, the β -sheet in LCAT is superhelically twisted, so that strand two and eight cross each other at an angle of approximately 60°. Clustering of the hydrophobic residues (red) in the core of LCAT, due to the packing of the amphipathic helices against the hydrophobic residues of the β -sheet, and distribution of hydrophilic residues at the surface of the molecule, are illustrated on the right part of Figure 7. The residues of the catalytic triad are in the typical configuration of the α/β hydrolase fold; the distance between the γ O of S181 and the N2 of H377 is 2.5 Å, while that between δ O of D345 and the N1 of H377 is 2.9 Å, comparable to the distances measured in crystallized lipases (Van Tilbeurgh et al., 1992, 1993). The backbone amides of the two oxyanion hole residues F103 and L182 involved in catalysis are located within 5 Å of each other.

The mode of interaction between LCAT and its phospholipid substrate is consistent with the model described above. Recent data by Wang and coworkers demonstrated that residue E149 contributes to the phospholipid substrate specificity of LCAT (Wang et al., 1997). A E149A mutation in human LCAT changes the fatty acid acyl chain specificity from 18:2 to 20:4. As this residue is located on the hydrophilic loop N-terminal of helix α 4–5, the E149A mutation probably facilitates the spatial accommodation of a more bulky arachidonic acid molecule in this cavity. Fatty acid binding to cutinase (Longhi et al., 1996), to *Rhizomucor miehei* lipase (Vasel et al., 1993; Norin et al., 1994), and to human pancreatic lipase (Van Tilbeurgh et al., 1992), involves similar interactions with a residue N-terminal of helix α 4–5. The accommodation of the cholesterol nucleus in LCAT can be predicted from the structural and functional homology between LCAT and *Candida cylindracea* cholesterol esterase (Ghosh et al., 1995), as both enzymes can function as an acyl transferase and as an esterase. The structural homology between LCAT and this esterase suggests that the cholesterol moiety would penetrate into LCAT from the N-terminal side of helices α 3–4 and α -His. The cholesterol molecule would, moreover, be situated outside the catalytic gorge and have few contacts with side-chain atoms. This model would thus be compatible with the low substrate specificity of LCAT, which esterifies different sterols as well as long-chain alcohols (Kitabatake et al., 1979).

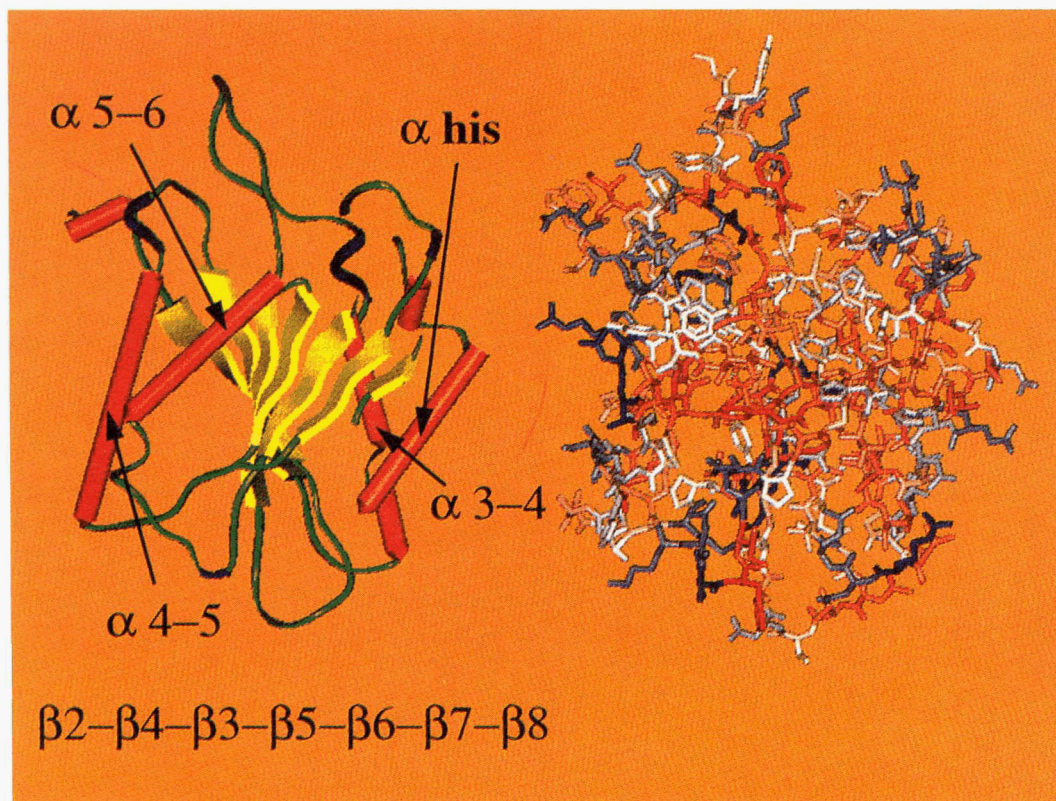


Fig. 7. Working model for the LCAT structure derived from the pancreatic lipase and *Candida antarctica* lipase coordinates, showing strands $\beta 2$ - $\beta 8$ (yellow), helices $\alpha(3-4)$, $\alpha(4-5)$, $\alpha(5-6)$, and α -His (red) and loops (green); right: same figure showing hydrophilic residues (blue) and hydrophobic residues (red).

Conclusion

We used the conserved features of the α/β hydrolase fold, previously identified during the 1995 IRBM Workshop (Hubbard et al., 1996), for identification of the catalytic residues of LCAT, for 3-D model building of the core and catalytic site, and for the prediction of functional domains in LCAT. A similar approach had been applied, for example, for the central domain of the bacterial enhancer-binding proteins (Osuna et al., 1997) and the ferroxidase family of proteins (Hansson et al., 1997). The construction of a limited number of mutants was sufficient to identify D345 and H377 as the catalytic residues of LCAT, together with F103 and L182 as the oxyanion hole residues. 3D model building by molecular modeling, using lipases as templates, further confirms that the proposed catalytic residues of LCAT lie in the right spatial configuration to allow esterase activity for LCAT. In analogy with lipases, we further identified a potential "lid" domain at residues 50-74 of LCAT, located N-terminal of the catalytic triad residues as in *Candida rugosa* lipase, which might be involved in the enzyme-substrate interaction.

Natural LCAT mutants resulting in either LCAT deficiency or FED are spread throughout the entire sequence from residue 10 to 399 (Kuivenhoven et al., 1997). Our 3D model clearly shows that these mutations are clustered in three distinct groups. The positioning of one group of FLD mutants, close to the catalytic triad, probably accounts for the observed loss of enzymatic activity. Our model further enables prediction of the LCAT domains involved in the interaction with the phospholipid substrate and can be applied to the design of mutants with specific substrate activity. This model awaits confirmation by X-ray crystallography of the LCAT enzyme.

Materials and methods

Homology calculations

Homology search of the SwissProt and PDB databanks using the BLAST algorithm (Altschul et al., 1990) was carried out on the server: <http://www.ncbi.nlm.nih.gov/BLAST/>. The secondary structure predictions methods were used from various www servers: the PHD method (Rost & Sander, 1993) at: <http://www.embl-heidelberg.de>, which uses a neural network scheme, the nn-predict program (Mehta et al., 1995; <http://www.cmpharm.ucsf.edu>), the SSP programs (Solovyev & Salamov, 1994; <http://dot.imgen.bcm.tcm.edu>); the SOPMA, Levin, DPM, and Gibrat methods (Geourjon & Deleage, 1994; <http://www.ibcp.fr>), which use a limited database of protein sequences for prediction of a given sequence.

The tertiary structure of LCAT was predicted using the threading approach of Jones, using the THREADER program (Jones et al., 1992, 1995), optimally fitting the sequence to each of a library of 556 protein folds derived from the database of protein structures. The "energy" of each possible fit was calculated by summing the proposed pairwise interactions. The lowest energy folds are then taken as the most probable matches. The 123D threading method was carried out using a sequence and secondary structure parameter of three and a contact capacity parameter of four (Alexandrov et al., 1996; <http://www-lmmb.nciferf.gov/~nicka/123D.html>). Results from the 3D Profile algorithm were obtained from the Fold Recognition Server at: <http://www.doe-mbi.ucla.edu/people/frsivr/submit.html>

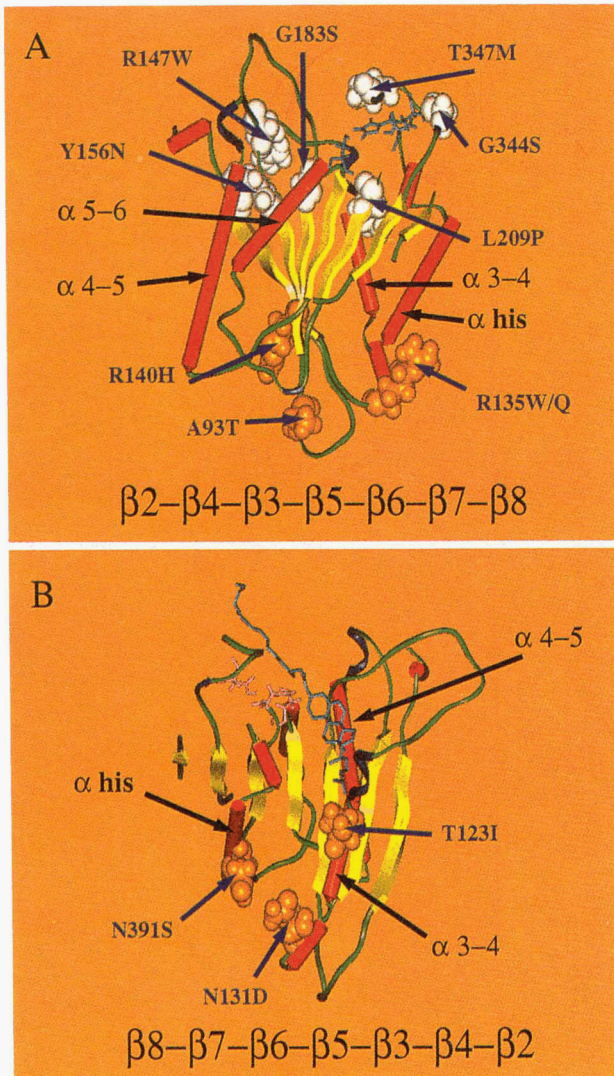


Fig. 8. Working model for the LCAT structure showing the location of natural FED and FLD mutants. **A:** FLD mutants: R147-W, Y156-N, G183-S, L209-P, G344-S, and T347-M are shown in white, A93-T, R135-W/Q, R140-H are shown in brown, catalytic residues are shown in blue. **B:** FED mutants T123-I, N131-D, and N391-S are shown in brown; the catalytic residues are shown in pink; a cholesterylester molecule is drawn in blue.

Site-directed mutagenesis

A plasmid vector, designated pXL 3105, allowing expression of LCAT in Cos-1 cells was constructed as follows: the complete LCAT coding sequence was excised from pXL2616 (Séguret-Macé et al., 1996), as an AvrII/BamHI fragment and was inserted together with a BglIII/KpnI fragment containing the SV40 polyA from pXL3094, into AvrII/KpnI-opened pXL3041. Mutagenesis was carried out using the Quick Change Site-Directed Mutagenesis method (Stratagene, France). In addition, a change in the restriction pattern was added to allow for easy evaluation. Mutations were built in by PCR using Pfu DNA polymerase. After DpnI digestion of the parental dam-methylated template, the synthesized mutated DNA was transformed into *E. coli* XL1-Blue supercompetent cells. Colonies were screened by restriction analysis and mutants were fully sequenced on a ALF automated sequencer (Pharmacia Biotech).

Transient expression of the LCAT cDNA in Cos-1 cells was carried out by transfection of subconfluent monolayers of the Cos-1 cells with a mixture of 16 μ g of the recombinant plasmids and 128 μ g of lipofectamine (Gibco) for 5 h. The cell culture media (Dulbecco's modified Eagle's medium, Life Technologies, Inc) were replaced after 16 h and harvested after 48 h.

LCAT activity and mass measurements

The activity of WT LCAT and mutants was tested on three different substrates: the α -activity was measured on a discoidal r-HDL substrate, consisting of 1-palmitoyl-2-linoleoyl phosphatidylcholine/cholesterol/apo A-I complexes, at a molar ratio of 100/10/1. The β -activity was measured on heat-inactivated LDL, isolated from human plasma by ultracentrifugation at densities between 1.03 and 1.063 g/mL. The amount of cholesteryl esters generated during the reaction was quantified by HPLC (Vercaemst et al., 1989; Vanloo et al., 1992). The phospholipase activity on a monomeric substrate was assayed using 1,2-bis-(1-pyrene-butanoyl)-sn-glycero-3-phosphocholine (Bonelli & Jonas, 1992). LCAT mass was assayed by solid-phase enzyme immunoassay using chicken antibodies specific to LCAT, and purified human LCAT as a standard, as follows: 100 μ L culture medium was coated onto titer plates for 3 h at 37°C and overnight at 4°C. A standard curve was constructed with purified rLCAT, at concentrations between 50 and 1,000 ng. Plates were washed and blocked and bound LCAT was detected by incubation with chicken anti-LCAT purified IgY at a concentration of 10 μ g/mL, followed by a peroxidase labeled rabbit anti-chicken IgY antibody. Bound peroxidase was incubated with a TMB substrate (Tetramethyl benzidine, Boehringer Mannheim, Germany), for 30 min. Incubation was stopped with H₂SO₄, and absorbance was read at 450 nm in the linear part of the standard curve. For Western blot analysis, equivalent volumes of media from cells expressing the normal or mutant LCAT were applied to the gel, which included molecular weight standards. The samples were separated on a 10% SDS-polyacrylamide gel and proteins were transferred onto a Immobilon membrane using a semi-dry blotting apparatus in a Tris (25 mM)-Glycine (192 mM) buffer at pH 8.3 containing 20% methanol. The bands were visualized using the chicken anti-LCAT antibody (purified IgY preparation) and a rabbit anti-chicken IgY coupled to peroxidase (Sigma) as second antibody using standard procedures. The bound peroxidase was visualized using the BM Chemiluminescence luminal substrate (Boehringer Mannheim, Germany).

Model building for LCAT

The working model for the N-terminal and the catalytic site of LCAT was built using the HOMOLOGY software (Biosym, San Diego, CA). The N-terminal part, between residues 73 and 210, which includes the active site Ser181, was built based upon the crystalline structure of human pancreatic lipase (1LPB). The design of the active site was further completed using the coordinates of the corresponding residues of the *Candida antarctica* lipase (1TCA). Loops were included whenever required between consecutive structural segments.

Acknowledgments

We are grateful to H. Pritchard (Vancouver) for the gift of the BHK cells, to B. Verheij (Univ. Utrecht) for helpful suggestions, and to C. Ampe

(Univ. Gent) for the use of the Biosym software. We acknowledge the excellent technical assistance of J. Taveirne and H. Caster. This work was supported by grant G-0061-96 of the Fund for Scientific Research-Flanders to J. Vandekerckhove and M. Rosseneu. F. Peelman is a recipient of a IWT doctoral Fellowship.

References

- Alexandrov NN, Nussinov R, Zimmer RM. 1996. Fast protein fold recognition via sequence structure alignment and contact capacity potentials. In: Hunter L, Klein TE eds. *Pacific Symp Biocomputing 96*. Singapore: World Scientific Press. pp 53–72.
- Altschul SF, Gish W, Miller W, Myers EW, Lipman DJ. 1990. Basic local alignment search tool. *J Mol Biol* 215:403–415.
- Bonelli FS, Jonas A. 1992. Continuous fluorescence assay for lecithin: Cholesterol acyltransferase using a water-soluble phosphatidylcholine. *J Lipid Res* 33:1863–1869.
- Cyglar M, Schrag JD, Sussman JL, Harel M, Silam N, Gentry MK, Doctor B. 1993. Relationship between sequence conservation and three-dimensional structure in a large family of esterases, lipases and related proteins. *Protein Sci* 2:366–382.
- Egloff MP, Marguet F, Buono G, Verger R, Cambillau C, van Tilbeurgh H. 1995. The 2.46 Å resolution structure of the pancreatic lipase-colipase complex inhibited by a C11 alkyl phosphonate. *Biochemistry* 34:2751–2762.
- Fisher D, Eisenberg D. 1996. Fold recognition using sequence-derived predictions. *Protein Sci* 5:947–955.
- Francone OL, Evangelista L, Fielding CJ. 1993. Lecithin-cholesterol acyltransferase: Effects of mutagenesis at N-linked oligosaccharide attachment sites on acyl acceptor specificity. *Biochim Biophys Acta* 1166:301–304.
- Francone OL, Evangelista L, Fielding JC. 1996. Effects of carboxy-terminal truncation on human lecithin: Cholesterol acyl transferase. *J Lipid Res* 37:1609–1615.
- Francone OL, Fielding CJ. 1991. Structure-function relationships of human lecithin cholesterol acyl transferase. Site directed mutagenesis at serine residues 181 and 216. *Biochemistry* 30:10074–10077.
- Geourjon C, Deleage G. 1994. A self-optimized method for protein secondary structure prediction. *Protein Eng* 7:157–164.
- Ghosh D, Wawrzak Z, Pletnev VZ, Li N, Kaiser R, Pangborn W, Jörnvall H, Erman M, Duax WL. 1995. Structure of uncomplexed and linoleate-bound *Candida cylindracea* cholesterol esterase. *Structure* 3:279–288.
- Glomset JA. 1968. The plasma lecithin: Cholesterol acyltransferase reaction. *J Lipid Res* 9:155–167.
- Hansson M, Gough SP, Brody SS. 1997. Structure prediction and fold recognition for the ferroxidase family of proteins. *Proteins Struct Funct Genet* 27:517–522.
- Hengstschlager-Ottad E, Kuchler K, Schneider WJ. 1995. Chicken lecithin-cholesterol acyl transferase. *J Biol Chem* 270:26139–26145.
- Hide WA, Chan L, Li W-H. 1992. Structure and evolution of the lipase superfamily. *J Lipid Res* 33:167–178.
- Higgins DG, Sharp PM. 1988. CLUSTAL: A package for performing multiple sequence alignment on a microcomputer. *Gene* 73:237–244.
- Hoeg JM, Vaisman BL, Demosky SJ Jr, Meyn SM, Talley GD, Hoyt RF, Feldman S, Berard AM, Sakai N, Wood D, Brousseau ME, Marcovina S, Brewer HB, Santamarina-Fojo S. 1996. Lecithin: Cholesterol acyltransferase overexpression generates hyperalpha-lipoproteinemia and a non-atherogenic lipoprotein pattern in transgenic rabbits. *J Biol Chem* 271:4396–4402.
- Hubbard T, Tramontano A, 1995 IRBM workshop team. 1996. Update on protein structure prediction: Results of the 1995 IRBM workshop. *Folding & Design* 1:R55–R63.
- Jauhainen M, Dolphin PJ. 1986. Human plasma lecithin cholesterol acyl transferase. An elucidation of the catalytic mechanism. *J Biol Chem* 261:7032–7043.
- Jauhainen M, Dolphin PJ. 1991. Human plasma lecithin cholesterol acyl transferase (LCAT). On the role of the essential carboxyl groups in catalysis. *Adv Exp Med Biol* 285:71–75.
- Jauhainen M, Ridgway N, Dolphin PJ. 1987. Aromatic boronic acids as probes of the catalytic site of human plasma lecithin cholesterol acyl transferase. *Biochim Biophys Acta* 918:175–188.
- Jauhainen M, Stevenson KJ, Dolphin PJ. 1988. Human plasma lecithin cholesterol acyl transferase. The vicinal nature of cysteine 31 and cysteine 184 in the catalytic site. *J Biol Chem* 263:6525–6533.
- Jonas A. 1991. Lecithin-cholesterol acyltransferase in the metabolism of high-density lipoproteins. *Biochim Biophys Acta* 1084:205–220.
- Jones DT, Miller RT, Thornton JM. 1995. Successful protein fold recognition by optimal sequence threading validated by rigorous blind testing. *Proteins Struct Funct Genet* 23:387–397.
- Jones DT, Taylor WR, Thornton JM. 1992. A new approach to protein fold recognition. *Nature* 359:86–89.
- Karmin O, Hill JS, Pritchard PH. 1995. Role of N-linked glycosylation of lecithin: Cholesterol acyltransferase in lipoprotein substrate specificity. *Biochim Biophys Acta* 1254:193–197.
- Kitabatake K, Piran U, Kamio Y, Doi Y, Nishida T. 1979. Purification of human lecithin: Cholesterol acyltransferase and its specificity towards the acyl acceptor. *Biochim Biophys Acta* 573:145–154.
- Kuivenhoven JA, Pritchard H, Hill J, Frohlich J, Assmann G, Kastelein J. 1997. The molecular pathology of lecithin cholesterol acyl transferase (LCAT) deficiency syndromes. *J Lipid Res* 38:191–205.
- Lee YP, Adimoolam S, Liu M, Subbaiah PV, Glenn K, Jonas A. 1997. Analysis of human lecithin-cholesterol acyltransferase activity by carboxyl-terminal truncation. *Biochim Biophys Acta* 1344:250–261.
- Lhose P, Chakrkh-Zadeh S, Lohse P, Seidel D. 1997. Human lysosomal acid lipase/cholesteryl ester hydrolase and human gastric lipase: Identification of the catalytically active serine, aspartic acid and histidine residues. *J Lipid Res* 38:892–903.
- Longhi S, Manesse M, Verheij M, De Haas G, Egmond M, Knoops-Mouthuy E, Cambillau C. 1996. Crystal structure of cutinase covalently inhibited by a triglyceride analogue. *Protein Sci* 6:275–286.
- Martinielle M, Holmquist M, Clausen IG, Patkar S, Svenden A, Hult K. 1996. The role of Glu87 and Trp89 in the lid of *Humicola lanuginosa* lipase. *Protein Eng* 9:519–524.
- Mehta PK, Heringa J, Argos P. 1995. A simple and fast approach to prediction of protein secondary structure from multiply aligned sequences with accuracy above 70%. *Protein Sci* 4:2517–2525.
- Norin M, Haefliger F, Achour A, Norin T, Hult K. 1994. Computer modeling of substrate binding to lipases from *Rhizomucor miehei*, *Humicola lanuginosa*, and *Candida rugosa*. *Protein Sci* 3:1493–1503.
- Ollis DL, Cheah E, Cyglar M, Dijkstra B, Frolow F, Franken S, Harel M, Remington SJ, Silman I, Schrag J, Sussman JL, Verschueren KHG, Goldman A. 1992. The α/β hydrolase fold. *Protein Eng* 5:197–211.
- Osuna J, Soberon X, Moret E. 1997. A proposed architecture for the central domain of the bacterial enhancer-binding proteins based on secondary structure prediction and fold recognition. *Protein Sci* 6:543–555.
- Richardson JS. 1981. The anatomy and taxonomy of protein structure. *Adv Prot Chem* 34:167–339.
- Rosseneu M, Peelman F, Vanloo B, Tavernier J, Vandekerckhove J. 1997. Identification of the catalytic triad and 3-D model building for LCAT. In: Fruchart JC, Brewer B, eds. *Abstract workshop on "Reverse cholesterol transport"*. Lille, October 3–4, 1997. p 10.
- Rost B, Sander C. 1993. Prediction of protein structure at better than 70% accuracy. *J Mol Biol* 232:584–599.
- Séguret-Macé S, Latta-Mahieu M, Castro G, Luc G, Fruchart JC, Rubin E, Denèfle P, Duverger N. 1996. Potential gene therapy for Lecithin-Cholesterol Acyltransferase (LCAT)-deficient and hypoalphalipoproteinemic patients with adenovirus-mediated transfer of human LCAT gene. *Circulation* 94:2177–2184.
- Solovyev VV, Salamon AA. 1994. Predicting α -helix and β -strand segments of globular proteins. *Comput Appl Biosci* 10:661–669.
- Sorci-Thomas M, Babiak J, Rudel LL. 1990. Lecithin-cholesterol acyltransferase (LCAT) catalyzes transacylation of intact cholesteryl esters. Evidence for the partial reversal of the forward LCAT reaction. *J Biol Chem* 265:2665–2670.
- Vanloo B, Taveirne J, Baert G, Lorent G, Vercaemst R, Lins L, Ruyschaert JM, Rosseneu M. 1992. Activation of Lecithin Cholesterol Acyl Transferase (LCAT) by the CNBr fragments of human apo AI and conversion of the discoidal complexes into spherical particles. *Biochim Biophys Acta* 1128:258–266.
- Van Tilbeurgh H, Egloff MP, Martinez C, Rugani N, Verger R, Cambillau C. 1993. Interfacial activation of the lipase-procolipase complex by mixed micelles revealed by X-ray crystallography. *Nature* 362:814–820.
- Van Tilbeurgh H, Sarda L, Verger R, Cambillau C. 1992. Structure of the lipase-colipase complex. *Nature* 359:159–161.
- Vasel B, Hecht HJ, Schmid R, Schomburg D. 1993. 3-D-structures of the lipase from *Rhizomucor miehei* at different temperatures and computer modelling of a complex of the lipase with triaryl glycerol. *J Biotechnology* 28:99–115.
- Vercaemst R, Union A, Rosseneu M. 1989. Separation and quantitation of free cholesterol and cholesteryl esters in a macrophage cell line by high performance liquid chromatography. *J Chrom* 494:43–52.
- Verhassel P, Aert R, Voet M, Volckaert G. 1994. Twelve open reading frames revealed in the 23.6 kb segment flanking the centromere on the *Saccharomyces cerevisiae* chromosome XIV right arm. *Yeast* 10:1355–1361.

- Wang JC, Gebre AK, Anderson RA, Parks JS. 1997. Amino acid residue 149 of lecithin cholesterol acyl transferase determines phospholipase A(2) and transacylase fatty acyl specificity. *J Biol Chem* 272:280-286.
- Wilmot CM, Thornton J. 1988. Analysis and prediction of the different types of beta-turns in proteins. *J Mol Biol* 203:221-232.
- Winkler FK, d'Arcy A, Hunziker W. 1990. Structure of human pancreatic lipase. *Nature* 343:771-774.
- Yang CY, Manoogian D, Pao Q, Lee FS, Knapp RD, Gotto AM, Pownall HJ. 1987. Lecithin: Cholesterol acyltransferase. *J Biol Chem* 262:3086-3091.